

## Self-Folding Cavitands

Dmitry M. Rudkevich, Göran Hilmersson, and Julius Rebek, Jr.\*

Contribution from The Skaggs Institute for Chemical Biology and The Department of Chemistry, The Scripps Research Institute, 10550 North Torrey Pines Road, La Jolla, California 92037

Received August 18, 1998

**Abstract:** A novel class of resorcinarene-based cavitands **2a–e** that fold into a deep ( $8 \times 10$  Å dimensions) open-ended cavity by means of intramolecular hydrogen bonds has been synthesized. As follows from the FTIR and  $^1\text{H}$  NMR spectral data in apolar solvent, a seam of eight intramolecular hydrogen bonds is stitched along the upper rim of the structure **2a–e**; the amide  $\text{C}=\text{O}\cdots\text{H}-\text{N}$  interactions bridge adjacent rings—interannular binding—and are held in place by the seven-membered intraannular hydrogen bonds. The self-folding in **2a–e** is reversibly controlled by solvent and temperature. Complexation of self-folding cavitands **2a–e** with organic molecules such as (1-substituted) adamantanes, lactams, and cyclohexane derivatives was demonstrated by  $^1\text{H}$  NMR spectroscopy in  $\text{CDCl}_3$ , benzene- $d_6$  and  $p$ -xylene- $d_{10}$ ; the binding energy  $-\Delta G^\circ$  values of 2–4 kcal  $\text{mol}^{-1}$  in  $p$ -xylene- $d_{10}$  at 295 K were calculated. The exchange between complexed and free guest species is slow on the NMR time-scale, and it is proposed that hydrogen bonds are responsible for these unique features. Employing the pronounced upfield  $^1\text{H}$  NMR shifts of the complexed guest molecules, attempts were made to study the structure of the caviplexes “from inside”, and the orientation of the encapsulated adamantanes **12**, **13**, as well as noncovalent interactions of complexed  $\epsilon$ -caprolactam **9b** with the host walls were deduced. Even though the guest-exchange process in **2a–e** is slow on the NMR time scale ( $k = 2 \pm 1 \text{ s}^{-1}$ ), it is still faster than that observed for the completely closed hydrogen-bonded calixarene-based capsules or for covalently sealed hemicarceplexes. This places them in an unusual position in the scale of cavity-containing receptors and opens new perspectives to use **2a–e** in catalysis and as  $^1\text{H}$  NMR supramolecular shift reagents.

## Introduction

Cavitands are synthetic structures with enforced cavities, molecular vessels capable of binding complementary organic compounds and ions.<sup>1</sup> They were first prepared by Cram from Högberg's resorcinarenes **1**,<sup>2</sup> and eventually were used in the syntheses of carcerands,<sup>3</sup> the closed-surface container molecules, velcands, the dimeric structures with large solvophobic surfaces,<sup>4</sup> and other molecular cavities.<sup>5</sup> The binding properties of cavitands have been examined in the solid state, the gas phase, in solution,<sup>1,6–8</sup> and even at an interface, self-assembled

monolayers have been presented on a gold surface.<sup>9</sup> We have been using cavitands to study encapsulation phenomena, the behavior of molecules temporarily isolated from bulk solution. These capsules involve reversibly formed calix[4]arene dimers<sup>10</sup> and the larger, deeper cylinders based on the resorcinarene cavitands.<sup>11</sup> The capsules are held together by a seam of *intermolecular* hydrogen bonds. These weak forces permit the assemblies to form and dissipate over a range of time scales and to encapsulate guests reversibly. Some phenomena that have emerged from the study of these systems are self-inclusion, pairwise selection of guest molecules,<sup>11</sup> and even chemical catalysis. In the present work, we explore the use of *intramolecular* hydrogen bonding and solvent effects to control the size

(1) (a) Moran, J. R.; Korbach, S.; Cram, D. J. *J. Am. Chem. Soc.* **1982**, *104*, 5826–5828. (b) Cram, D. J.; Korbach, S.; Kim, H.-E.; Knobler, C. B.; Maverick, E. F.; Ericson, J. L.; Helgeson, R. C. *J. Am. Chem. Soc.* **1988**, *110*, 2229–2237. (c) Tunstad, L. M.; Tucker, J. A.; Dalcanele, E.; Weiser, J.; Bryant, J. A.; Sherman, J. C.; Helgeson, R. C.; Knobler, C. B.; Cram, D. J. *J. Org. Chem.* **1989**, *54*, 1305–1312. (d) Cram, D. J. *Science* **1983**, *219*, 1177–1183. (e) Cram, D. J.; Cram, J. M. *Container Molecules and their Guests*; Royal Society of Chemistry: Cambridge, 1994, pp 85–130.

(2) (a) Högberg, A. G. S. *J. Am. Chem. Soc.* **1980**, *102*, 6046–6050. (b) Högberg, A. G. S. *J. Org. Chem.* **1980**, *45*, 4498–4500. For a timely review see: Timmerman, P.; Verboom, W.; Reinhoudt, D. N. *Tetrahedron* **1996**, *52*, 2663–2704.

(3) For a review, see: Sherman, J. C. *Tetrahedron* **1995**, *51*, 3395–3422. See also ref 1e, pp 131–216.

(4) Cram, D. J.; Choi, H.-J.; Bryant, J. A.; Knobler, C. B. *J. Am. Chem. Soc.* **1992**, *114*, 7748–7765.

(5) (a) Timmerman, P.; Nierop, K. G. A.; Brinks, E. A.; Verboom, W.; van Veggel, F. C. J. M.; van Hoorn, W. P.; Reinhoudt, D. N. *Chem. Eur. J.* **1995**, *1*, 132–143. (b) Higler, I.; Timmerman, P.; Verboom, W.; Reinhoudt, D. N. *J. Org. Chem.* **1996**, *61*, 5920–5931. (c) Higler, I.; Verboom, W.; van Veggel, F. C. J. M.; de Jong, F.; Reinhoudt, D. N. *Liebigs Ann./Recueil* **1997**, 1577–1586.

(6) (a) Cram, D. J.; Stewart, K. D.; Goldberg, I.; Trueblood, K. N. *J. Am. Chem. Soc.* **1985**, *107*, 2574–2575. (b) Tucker, J. A.; Knobler, C. B.; Trueblood, K. N.; Cram, D. J. *J. Am. Chem. Soc.* **1989**, *111*, 3688–3699.

(7) (a) Dalcanele, E.; Soncini, P.; Bacchilega, G.; Ugozzoli, F. *J. Chem. Soc., Chem. Commun.* **1989**, 500–502. (b) Soncini, P.; Bonsignore, S.; Dalcanele, E.; Ugozzoli, F. *J. Org. Chem.* **1992**, *57*, 4608–4612. (c) Dalcanele, E.; Costantini, G.; Soncini, P. *J. Inclusion Phenom. Mol. Recognit. Chem.* **1992**, *13*, 87–92.

(8) Gas-phase complexation studies: (a) Vincenti, M.; Dalcanele, E.; Soncini, P.; Guglielmetti, G. *J. Am. Chem. Soc.* **1990**, *112*, 445–447. (b) Vincenti, M.; Minero, C.; Pelizzetti, E.; Secchi, A.; Dalcanele, E. *Pure Appl. Chem.* **1995**, *67*, 1075–1084. (b) Dickert, F. L.; Baumler, U. P. A.; Stathopoulos, H. *Anal. Chem.* **1997**, *69*, 1000–1005.

(9) (a) Schierbaum, K. D.; Weiss, T.; Thoden van Velzen, E. U.; Engbersen, J. F. J.; Reinhoudt, D. N.; Gopel, W. *Science* **1994**, *265*, 1413. (b) Huisman, B.-H.; Rudkevich, D. M.; van Veggel, F. C. J. M.; Reinhoudt, D. N. *J. Am. Chem. Soc.* **1996**, *118*, 3523–3524.

(10) (a) Shimizu, K. D.; Rebek, J., Jr. *Proc. Natl. Acad. Sci. USA* **1995**, *92*, 12403–12407. (b) Hamman, B. C.; Shimizu, K. D.; Rebek, J., Jr. *Angew. Chem., Int. Ed. Engl.* **1996**, *35*, 1326–1330. (c) Castellano, R. K.; Rudkevich, D. M.; Rebek, J., Jr. *J. Am. Chem. Soc.* **1996**, *118*, 10002–10003. (d) Castellano, R. K.; Rudkevich, D. M.; Rebek, J., Jr. *Proc. Natl. Acad. Sci. U.S.A.* **1997**, *94*, 7132–7137.

(11) (a) Heinz, T.; Rudkevich, D. M.; Rebek, J., Jr. *Nature* **1998**, *394*, 764–766. (b) Ma, S.; Rudkevich, D. M.; Rebek, J., Jr. *J. Am. Chem. Soc.* **1998**, *120*, 4977–4981.

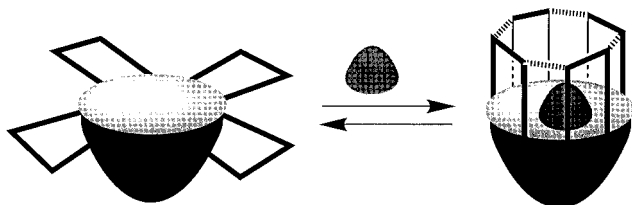


**Figure 1.** Schematic representation of the concept of reversibly self-folding cavitands. Dashed lines indicate sites of intramolecular hydrogen bonds.

and shape of cavitands, their folding and unfolding behavior, and their binding of complementary guests (Figure 1). The complexes of such self-folding cavitands, the caviplexes, feature unusually high kinetic stability in solution, and we interpret their behavior through the effects of hydrogen bonding on the host's conformational dynamics.<sup>12,13</sup>

## Results and Discussion

In Högberg's resorcinarenes **1** (Figure 2), the eight hydroxy groups form intramolecular hydrogen bonds, and these interactions rigidify the structure by stabilizing the  $C_{4v}$  cone conformation.<sup>14</sup> When the OH hydrogens are substituted, the flexibility of the resorcinarene skeleton increases, and conformations with other symmetries become preferred.<sup>2</sup> Condensation with (hetero)aryl halides builds up the walls on the rim of the macrocyclic structure and creates the cavitands and velcrams. The conformational dynamics of these molecules have been thoroughly described by Cram.<sup>4,15</sup> The molecule flutters between  $C_{4v}$  and  $C_{2v}$  symmetries. The former is preferred at higher temperatures and has all four walls up; it features a well-defined, vase-like shape. The latter has these walls flipped outward in a kite-like shape and is the dominant conformation below room temperature. The barrier to interconversion is typically 10–12 kcal/mol for cavitands with unsubstituted resorcinols and 17–19 kcal/mol with 2'-alkylated ones.<sup>4,15</sup>

We prepared new variants, cavitands **2a–e**, functionalized with eight secondary amides at the upper rim of the molecule (Figure 2). Molecular modeling<sup>16</sup> indicated that the vicinal secondary amides could form intramolecular hydrogen bonds through a seven-membered ring (Figure 3). In octaamides **2a–e** hydrogen bonds can also bridge adjacent rings. The result is a deepened vase, and the walls form a stall and forestall the conformational change to the kite. Both <sup>1</sup>H NMR and FTIR spectroscopy, described below, support the role of these intramolecular hydrogen bonds in these self-folding cavitands **2a–e** and determine the unusual complexation properties of these molecules.

(12) Preliminary publication: Rudkevich, D. M.; Hilmersson, G.; Rebek, J., Jr. *J. Am. Chem. Soc.* **1997**, *119*, 9911–9912. Mass spectrometric characterization of the ion-labeled complexes will be published elsewhere.

(13) A cyclic array of cooperative intramolecular hydrogen bonds is somewhat responsible for the structure of valinomycin, a natural ionophore, and its complexes with cations, see: Dobler, M. In *Comprehensive Supramolecular Chemistry*; Gokel, G. W., Ed.; Pergamon: Elmsford, NY, 1996; p 267–313.

(14) (a) Abis, L.; Dalcanale, E.; Du vosel, A.; Spera, S. *J. Org. Chem.* **1988**, *53*, 5475–5479. (b) Aoyama, Y.; Tanaka, Y.; Sugahara, S. *J. Am. Chem. Soc.* **1989**, *111*, 5397–5404. (c) Abis, L.; Dalcanale, E.; Du vosel, A.; Spera, S. *J. Chem. Soc., Perkin Trans. 2* **1990**, 2075–2080. For X-ray studies, see also ref 1c and Hibbs, D. E.; Hursthouse, M. B.; Malik, K. M. A.; Adams, H.; Stirling, C. J. M.; Davis, F. *Acta Crystallogr.* **1998**, *C54*, 987–992.

(15) Moran, J. R.; Ericson, J. L.; Dalcanale, E.; Bryant, J. A.; Knobler, C. B.; Cram, D. J. *J. Am. Chem. Soc.* **1991**, *113*, 5707–5714.

(16) Mohamadi, F.; Richards, N. G.; Guida, W. C.; Liskamp, R.; Lipton, M.; Caufield, C.; Chang, G.; Hendrickson, T.; Still, W. C. *J. Comput. Chem.* **1990**, *11*, 440–467.

**Synthesis.** Resorcinarenes **1a,c**, and their 2'-methyl derivative **1b** were coupled with 1,2-difluoro-4,5-dinitrobenzene<sup>17</sup> in DMA in the presence of Et<sub>3</sub>N with the formation of bright yellow octanitro compounds **4a,b**, and **c** in 25–40% yields (Scheme 1). Reduction of the octanitro derivatives with SnCl<sub>2</sub>·2H<sub>2</sub>O in boiling EtOH and concentrated HCl afforded the relatively unstable and oxygen-sensitive octaamines. Subsequent acylation with appropriate acyl chlorides under Schotten–Baumann conditions in EtOAc–H<sub>2</sub>O in the presence of K<sub>2</sub>CO<sub>3</sub> gave octaamides **2a–e** and **5** as colorless solids (Scheme 1).<sup>18</sup> From this reaction the incompletely acylated products, heptaamides **6a,b**, were also isolated and characterized. Model compounds **7a,b** for spectroscopic comparisons were prepared by acylation of 1,2-diamino-4,5-dimethoxybenzene<sup>19</sup> with octanoyl and chloroacetyl chloride, respectively. Cavitand **3** (R = (CH<sub>2</sub>)<sub>10</sub>CH<sub>3</sub>) was synthesized for comparison purposes from resorcinarene **1a** and 2,3-dichloroquinoline following the published procedure.<sup>7</sup>

## Spectroscopic Properties and Conformational Behavior.

All three octanitro compounds **4a–c** are clearly  $C_{2v}$  conformers at room temperature, and their <sup>1</sup>H NMR spectra possess, in particular, two sets of aromatic resonances (see Experimental Section). At >330 K, however, **4a** and **c** undergo transformation to the  $C_{4v}$  conformer (in CDCl<sub>3</sub>). In contrast, the <sup>1</sup>H NMR spectra of octaamides **2a–e** in various nonpolar solvents showed the spectroscopic earmarks of the  $C_{4v}$  conformation<sup>15</sup> at room temperature, including the characteristic methine CH triplet at ca. 6 ppm (Figure 4). The N–H resonances for **2a–e** are far downfield, and the FTIR spectroscopic data also suggest strong hydrogen bonding (Table 1). Of particular interest are the two amide NH singlets found in the <sup>1</sup>H NMR spectra of **2a,b,d,e** in apolar solvents (Table 1).<sup>20,21</sup> The two amides present hydrogen bonds that can bridge adjacent rings—*interannular* binding—and are held in place by the seven-membered *intraannular* hydrogen bonds (Figure 5). One of the hydrogen bonds is less sensitive to temperature and is shielded from external solvent, whereas the other is somewhat more exposed to the solvent. The two N–H signals coalesce at higher temperatures. The amides provide a head-to-tail seam of intramolecular hydrogen bonds along the upper rim of the structure **2a–e**. These hydrogen bonds are coherent and may offer each other the added benefits of cooperativity.<sup>22,13</sup>

In media more competitive for hydrogen bonds (DMSO-*d*<sub>6</sub>–CDCl<sub>3</sub> or DMSO-*d*<sub>6</sub>-*p*-xylene-*d*<sub>10</sub> mixtures) the signals for the

(17) Kazimierzczuk, Z.; Dudycz, L.; Stolarski, R.; Shugar, D. *Nucleosides Nucleotides* **1981**, *8*, 101–117.

(18) We also prepared and characterized (<sup>1</sup>H NMR, HRMS-FAB) the corresponding octakis(tolylsulfonylamides) by reduction of **4a,b** and subsequent acylation with TsCl in dry pyridine, evaporation, and precipitation with cold MeOH. Their <sup>1</sup>H NMR spectra in CDCl<sub>3</sub> and benzene-*d*<sub>6</sub> showed similar behavior as for **2a–e** and **5**, respectively. However, no complexation with lactams and monosubstituted adamantanes was detected by <sup>1</sup>H NMR spectroscopy.

(19) Zhou, Z.-L.; Weber, E.; Keana, J. F. W. *Tetrahedron Lett.* **1995**, *36*, 7583–7586 and references therein.

(20) Cavitand **2c**, functionalized with eight chloroacetyl amido groups, exhibits only one amide NH singlet at 295 K in CDCl<sub>3</sub> and benzene-*d*<sub>6</sub>. At low temperatures in CDCl<sub>3</sub>, the N–H singlet broadened then separated ( $T_c \approx 235$  K), and at temperatures lower 230 K two N–H signals were clearly observed. No coalescence was observed for model, nonmacrocyclic compound **7b** up to 215 K in CDCl<sub>3</sub>. Such a spectroscopic behavior of **2c** implies the fast interconversion between the amide sites on the NMR time scale at room temperature.

(21) The barrier to interconversion ( $\Delta G^\ddagger$ ) of the two types of N–H signals is  $17.4 \pm 0.5$  kcal mol<sup>-1</sup> ( $T_c \approx 87$  °C) in toluene-*d*<sub>8</sub> and *p*-xylene-*d*<sub>10</sub>, see ref 12.

(22) For a detailed discussion of cooperative interactions involving amides, see: (a) Guo, H.; Karplus, M. *J. Phys. Chem.* **1994**, *98*, 7104–7105. (b) Bisson, A. P.; Hunter, C. A.; Morales, J. C.; Young, K. *Chem. Eur. J.* **1998**, *4*, 845–851.

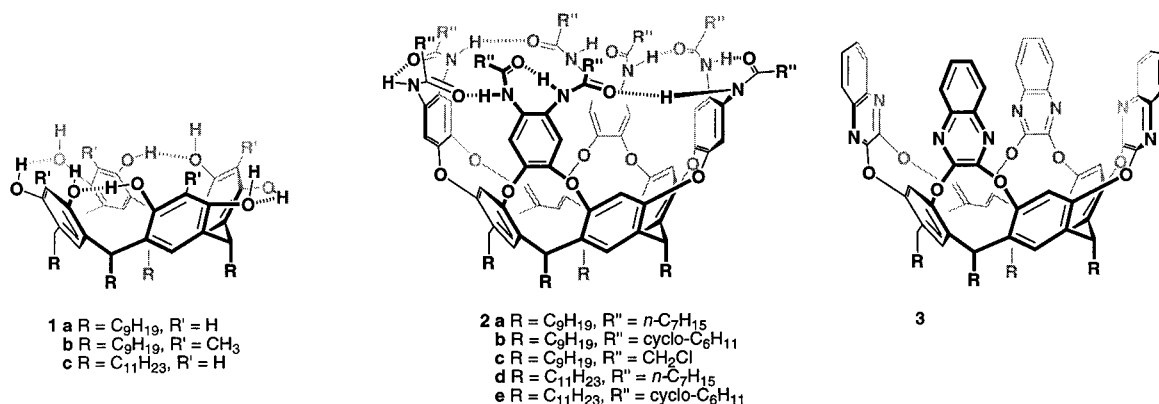


Figure 2. Högborg's resorcinarenes **1** and derived cavitands **2** and **3**.

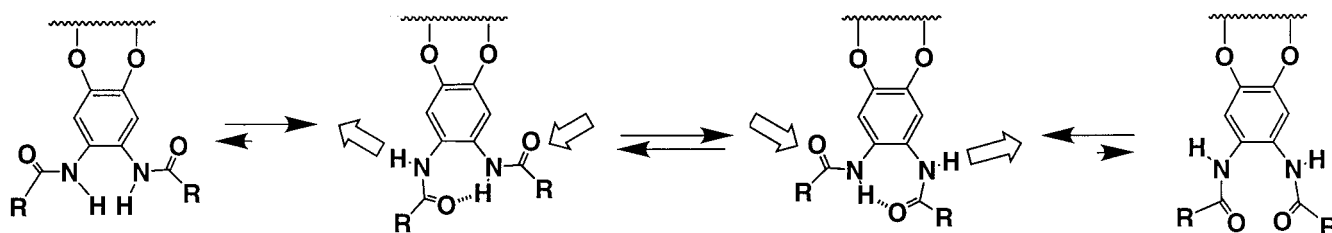
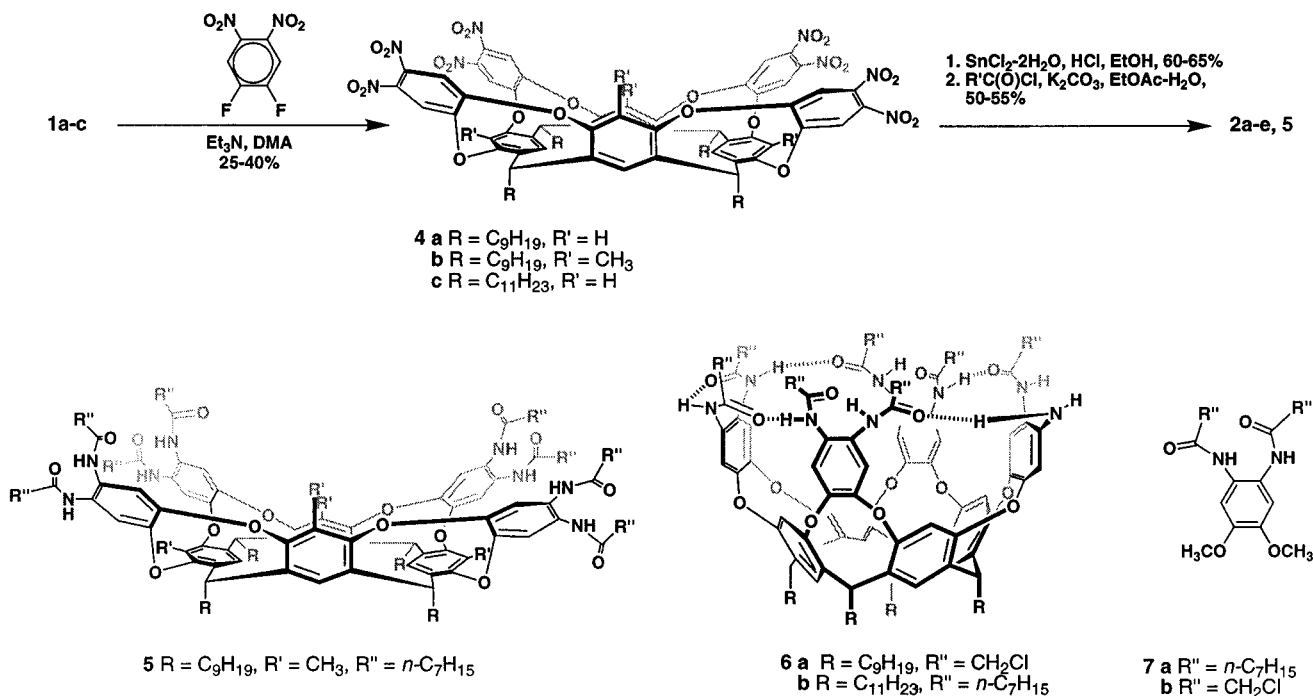


Figure 3. Intramolecular hydrogen bonding in vicinal diamides, used for the synthesis of self-folding cavitands **2a–e**. The self-complementary donor and acceptor sites are indicated.

#### Scheme 1



“upper” end of the molecule, for example, the NH singlets and the diamido aromatics, are broad, indicating a dynamic process, which is probably the  $C_{4v}$  to  $C_{2v}$  interconversion.

For the model compounds **7a,b** (Scheme 1, Table 1), a single N–H resonance upfield 8.7 ppm was observed in nonpolar solvents at room temperature. The N–H signal is much more sensitive to temperature, and it is more concentration dependent (<sup>1</sup>H NMR, FTIR).<sup>12</sup> Obviously, the model **7a,b** undergo fast exchange between two intramolecular hydrogen-bonded structures, and at increased concentrations, intermolecular aggregates can be formed (see also Figure 3).

Compound **5** that is based on 2'-methylresorcinarene **1b**, is

a  $C_{2v}$  conformer at room temperature and exhibits two sets of aromatic and 2'-Me protons in the <sup>1</sup>H NMR spectra in different solvents. The amide sites are remote from each other and there is no hydrogen bonding between adjacent aromatic rings. Accordingly, octaamide **5** has spectroscopic characteristics that are very similar to those of the model **7a** (Table 1).

Additional evidence of the cyclic array of hydrogen bonds in **2a–e** comes from symmetry considerations. Due to the head-to-tail nature (either clockwise or counterclockwise) of the hydrogen-bonding pattern in apolar solvents, the C(O)CH<sub>2</sub> protons in **2a–e**, but not in **7a,b**, become diastereotopic (Figure 6A). In the case of octakis(chloroacetamido) cavitand **2c**, this



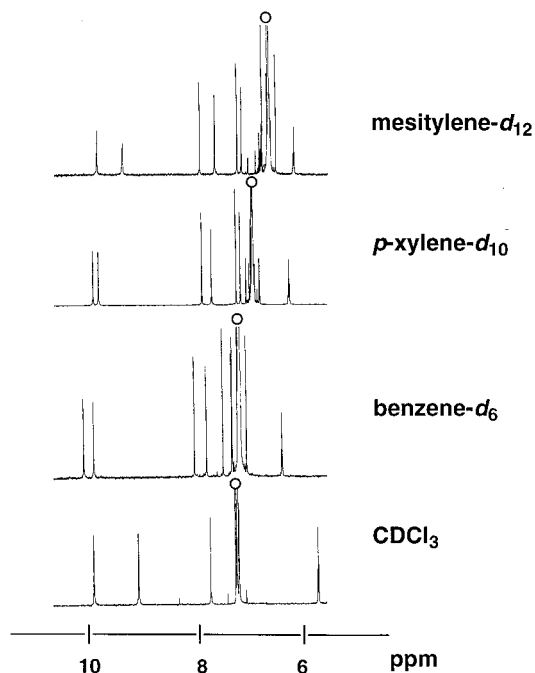


**Figure 4.** Downfield region of the  $^1\text{H}$  NMR spectra (600 MHz, 295 K) of cavitant **2d** (0.5 mM) in different solvents. The solvent signals with corresponding satellites are marked.

**Table 1.** Spectroscopic Data for the Amide NH Signals in Cavitanes **2c,d,e** and **5**, and Model Compounds **7a,b** in Various Solvents<sup>a,b</sup>

	solvent	$\delta$ , ppm	$\nu$ , $\text{cm}^{-1}$
<b>2c</b>	$\text{CDCl}_3$	9.5	3253
	benzene- $d_6$	9.6	
	$p$ -xylene- $d_{10}$	9.4	
	benzene- $d_6$ -DMSO- $d_6$ , 10:1	9.7	
<b>2d</b>	$\text{CDCl}_3$	9.9, 9.1	3240
	benzene- $d_6$	10.1, 9.9	3233
	toluene- $d_8$	10.2, 10.0	
	$p$ -xylene- $d_{10}$	10.0, 9.8	
	mesitylene- $d_{12}$	9.8, 9.3	
	$\text{CDCl}_3$ -DMSO- $d_6$ , 10:1	9.1	
<b>2e</b>	$\text{CDCl}_3$	9.7, 8.8	3246
	benzene- $d_6$	9.8, 9.4	
	$p$ -xylene- $d_{10}$	9.6, 9.5	
<b>5</b>	$\text{CDCl}_3$	7.9, 7.8	3419, 3255
	benzene- $d_6$	9.0 br, 8.3 br	
	$\text{CDCl}_3$ -DMSO- $d_6$ , 1:10	9.2, 9.1	
<b>7a</b>	$\text{CDCl}_3$	8.7 <sup>d</sup>	3421, 3309 w
	benzene- $d_6$	8.5 <sup>d</sup>	3389, 3254 w
	DMSO- $d_6$	9.2	
<b>7b</b>	$\text{CDCl}_3$	8.5 <sup>d</sup>	

<sup>a</sup> At 0.5 mM,  $295 \pm 1$  K. <sup>b</sup> Spectra of cavitanes **2a** and **b** are similar to those of **2d** and **e**, respectively. <sup>c</sup> The spectra are essentially concentration independent (20–0.05 mM); error  $\pm 0.1$  ppm. <sup>d</sup> At 20 mM. The IR absorption ratios change in the expected concentration-dependent manner toward the monomer upon dilution from 20 to 0.05 mM. br - broad signal, w - weak absorption.

results in a large geminal coupling constant of 13.7 Hz in  $\text{CDCl}_3$  and benzene- $d_6$  (Figure 6B). As expected, addition of 5–10% (vol) of highly competitive DMSO- $d_6$  breaks this circle of hydrogen bonds, and the  $\text{C}(\text{O})\text{CH}_2\text{Cl}$  AB-system collapses into a singlet (Figure 6B). In the same way, the two hydrogen-bonded amide NH singlets in **2a,b,d**, and **e** become one singlet upon DMSO- $d_6$  addition. Similar behavior was detected in some calixarene-based capsules which feature head-to-tail cyclic patterns of urea groups.<sup>10</sup>

Even the heptaamides **6a,b** exist in a vase conformation at  $\geq 295$  K. The  $^1\text{H}$  NMR spectra of **6a,b** in  $\text{CDCl}_3$  and benzene-

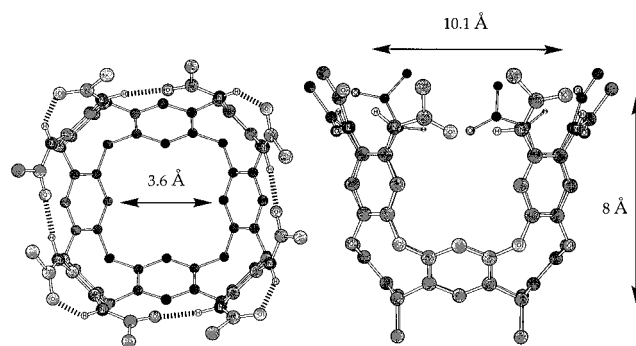


**Figure 5.** Two views of the energy-minimized<sup>16</sup> structure of cavitant **2**; the long alkyl chains and CH hydrogens are omitted for viewing clarity.

$d_6$  show, in particular, seven distinct downfield amide NH resonances within 10–8 ppm region and four CH methine triplets at ca. 6 ppm. Obviously, a seam of cooperative hydrogen bonds still exists, although the cycle is broken. The lone amino group can act as a donor to the nearby carbonyls but not as an acceptor to the nearby N–H bonds.

**Complexation.** Complexation properties of previously known cavitanes (alkylenedioxy-bridged, dialkylsilicon-bridged and heterophenylene-bridged) have been studied in great detail by Cram and Dalcanale.<sup>6–8</sup> In solution, the affinity toward small organic molecules was detected, but the complexation processes are fast on the NMR time scale, and only time-averaged signals can be seen when binding occurs. In the case of alkylenedioxy-bridged cavitanes, chemical shift changes of up to 0.28 ppm were detected in  $\text{CCl}_4$  upon addition of (5% vol)  $\text{CD}_2\text{Cl}_2$ ,  $\text{CD}_3\text{-CN}$ ,  $\text{CS}_2$ ,  $\text{CD}_3\text{NO}_2$ , and  $\text{C}_6\text{D}_5\text{CD}_3$ . The association constant ( $K_{\text{ass}}$ ) of  $\leq 100 \text{ M}^{-1}$  was calculated for  $\text{CD}_3\text{CN}$  at 300 K.<sup>6</sup> Heterophenylene-bridged cavitanes (for example, **3**) showed affinity toward aromatic molecules;  $K_{\text{ass}}$  of up to  $200 \text{ M}^{-1}$  were found in acetone- $d_6$ .<sup>7</sup> We found that self-folding in cavitanes **2a–e** results in a number of novel features. First, the amide groups deepen the cavity to dimensions of ca.  $8 \times 10 \text{ \AA}$  (Figure 5). Second, the size and shape of the deep cavity very much resembles those of known<sup>7,15</sup> cavitant **3**. However, in contrast to **3**, the cavities in **2a–e** are formed under thermodynamic control. Third, exchange between complexed and free guest species was slow on the NMR time-scale. We propose that the circle of hydrogen bonds is responsible for these features. Initially, we tested the behavior of **2a–e** in aromatic solvents. Undoubtedly, the deep but open-ended cavity is solvated, and molecular modeling<sup>16</sup> accommodates one molecule of  $p$ -xylene or mesitylene and, at best, two molecules of benzene or  $\text{CHCl}_3$  inside. The solvent mixtures benzene- $d_6$ - $\text{CDCl}_3$ , benzene- $d_6$ - $p$ -xylene- $d_{10}$ , or benzene- $d_6$ -toluene- $d_8$  give only one set of  $^1\text{H}$  NMR signals at 25 °C.

Intuitively, it seemed that polycyclic alkanes, such as adamantanes, and structures with hydrogen-bonding capabilities, such as lactams, would have the right size and shape to fill the cavity in **2a–e**, and indeed, such complexes were detected. Specifically, addition of excess *N*-cyclohexyluracil **8**, several cyclic lactams (**9a–c**, **10**, **11**, and **14**), or adamantane and its amino and carboxy derivatives (**12** and **13**, Figure 7) to a solution of **2** in benzene- $d_6$  and  $p$ -xylene- $d_{10}$  gave two sets of signals in the  $^1\text{H}$  NMR spectra, both for the cavitanes and the corresponding cavitplexes (Figures 8–10). The signals for the guest species were clearly observed *upfield* of 0 ppm, a feature characteristic of inclusion in a shielded environment and similar to the shifts observed in covalently bound carceplexes.<sup>3</sup> However, ferrocene, (*1R*)-(–)-camphorquinone, some Kemp's

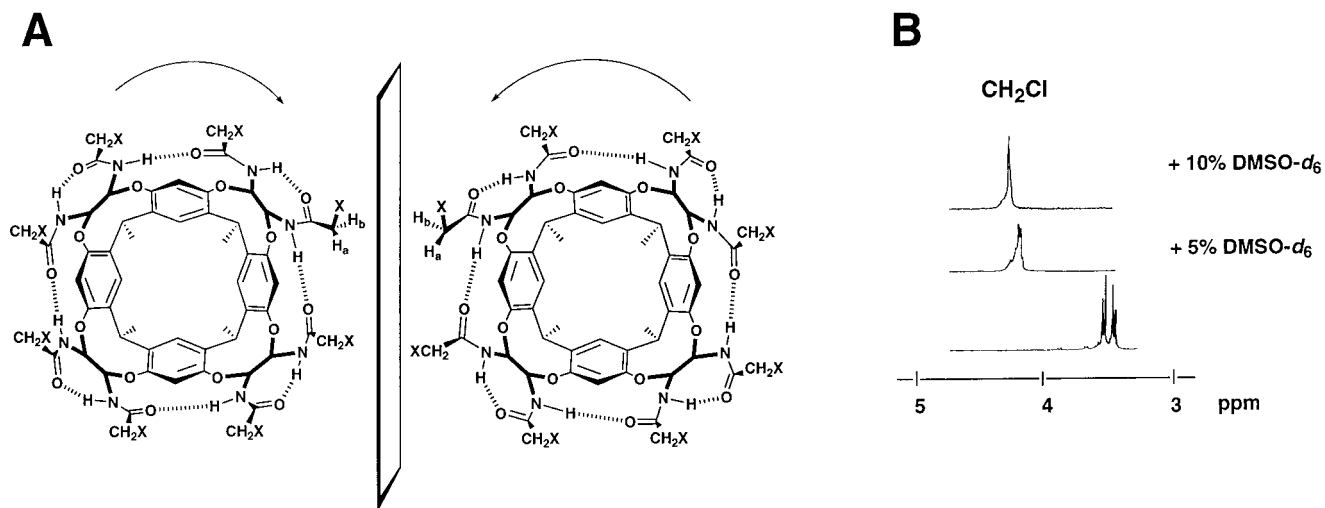


**Figure 6.** (A) Schematic depiction of the enantiomers caused by the head-to-tail cyclic array of hydrogen-bonded amides in compounds **2a–e**. (B) Region of the  $^1\text{H}$  NMR spectra (600 MHz, 295 K) of compound **2c** in benzene- $d_6$  (ca 0.5 mM) and in benzene- $d_6$ –DMSO- $d_6$  mixtures.

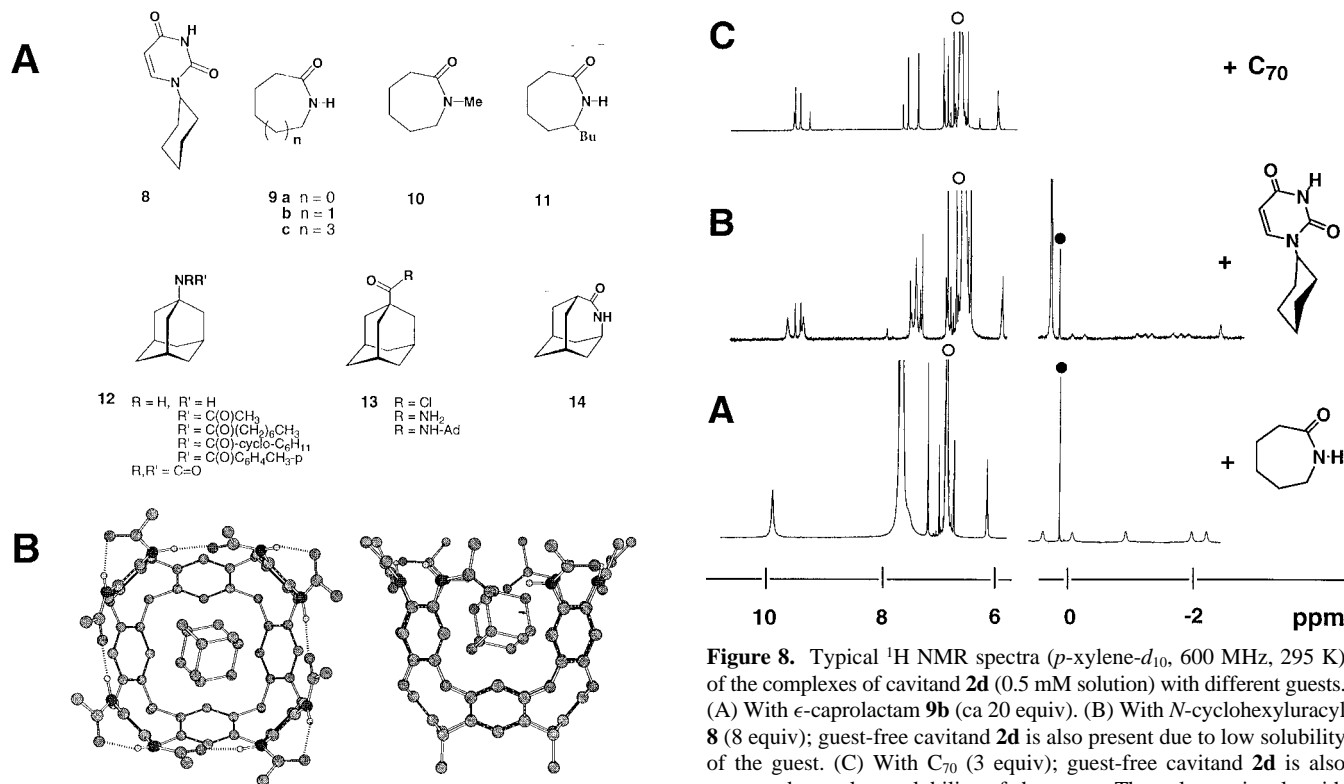


**Figure 7.** (A) Guest molecules **8–14** used for complexation with cavitands **2a–e**. (B) Energy-minimized<sup>16</sup> complex of **2** with adamantane. Long alkyl chains, CH hydrogens and the rear of the structure have been deleted for clarity.

triacid derivatives, 2(1*H*)-pyridone, 2-pyrrolidinone, and valerolactam showed no kinetically stable complexes with **2** in the  $^1\text{H}$  NMR spectra in either benzene- $d_6$  or *p*-xylene- $d_{10}$ .

The NMR signals of the cavitand skeleton, especially the aromatics and the amide NH groups, also undergo significant changes upon complexation (Figures 8–10). In contrast, cavitand **3** ( $\text{R} = (\text{CH}_2)_{10}\text{CH}_3$ ) does *not* show such a behavior; only slight changes in the chemical shifts of the host aromatics were observed, and no encapsulated guest species were detected in different titration experiments with  $\epsilon$ -caprolactam and adamantanes.

Of particular interest is the formation of a complex between  $\text{C}_{70}$  and **2** in *p*-xylene- $d_{10}$  solution. Although molecular modeling

indicates that the cavity in **2** is unable to accommodate such a sizable molecule, addition of up to 3 equiv of  $\text{C}_{70}$  to a solution of **2d** (0.5–0.8 mM concentration) gave *two* sets of signals in the  $^1\text{H}$  NMR spectra (Figure 8C). From the integration, the association constant  $K_{\text{ass}}$  value of  $400 \pm 100 \text{ M}^{-1}$  was estimated, assuming 1:1 complexation at 295 K. However, the corresponding Job plots also indicate the presence of the 2:1 **2d**· $\text{C}_{70}$  complex. Due to the low solubility of  $\text{C}_{70}$  in xylene, the equilibria cannot be completely driven to the complex formation. Even so, this appears to be a rare example of a *kinetically* stable complex between  $\text{C}_{70}$  and synthetic receptor in an organic solvent.<sup>23,24</sup>

The sharp and widely separated signals for free and bound guest species indicate substantial energetic barriers for guest

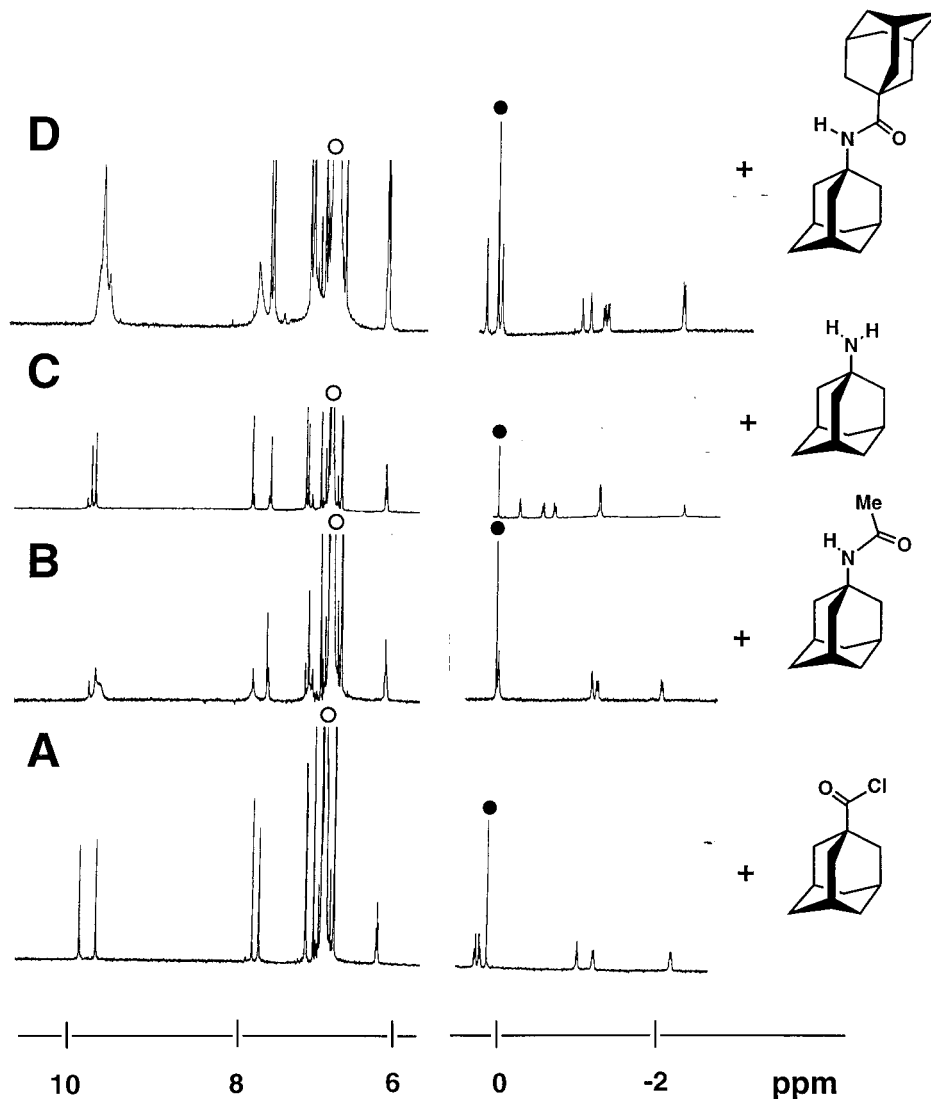


**Figure 9.** Downfield and upfield regions of the  $^1\text{H}$  NMR spectra (*p*-xylene- $d_{10}$ , 600 MHz, 295 K) of cavitand **2d** during complexation with 1-substituted adamantanes. (A) With 1-adamantanecarbonyl chloride. (B) With *N*-(1-adamantyl)acetamide; residual signals of guest-free cavitand **2d** are also present due to weak complexation. (C) With 1-adamantanamine. The furthest upfield signal (ca.  $-2$  ppm) is due to the  $\text{NH}_2$  resonance; guest-free cavitand **2d** is also present due to weak complexation. (D) With 1-[*N*-(1-adamantyl)]adamantanecarboxamide; two different complexes are present. The solvent signals with corresponding satellites and the internal standard singlet are marked as before. The host and guest concentrations are 0.5 and  $\geq 25$  mM, respectively.

exchange in and out of the vases **2a–e**. The process is *slow* on the NMR time scale at room temperature, a behavior for open-cavity receptors that is unprecedented.<sup>25</sup> In the preliminary publication of these observations, it was proposed that the solvent replacement by the guest takes place through an unfolding of the cavity, for example the seam of hydrogen bonds must be (partly) broken to release the solvent.<sup>12</sup> To support this mechanism, an EXSY experiment on the adamantane complex with **2d** in *p*-xylene- $d_{10}$  was performed (see Experimental

Section). The activation barrier ( $\Delta G^\ddagger$ ) for the exchange between the free and complexed guest of  $16.9 \pm 0.4$  kcal mol $^{-1}$  at 295 K was found; the exchange rate constant  $k = 2 \pm 1$  s $^{-1}$  was calculated. This barrier is almost the same as the interconversion barrier between the two amide signals,<sup>21</sup> and we still interpret this as no coincidence. Rather, the processes, unfolding and guest exchange, are inextricably connected.

It was unexpected to find that an open-ended vessel could so effectively desolvate and shield guest species from the environment of the bulk solution. The significant upfield  $^1\text{H}$

(23) The UV–vis spectra in *p*-xylene at 295 K showed the broad absorbance increase at 400–600 nm upon titrating the  $\text{C}_{70}$  solution ( $10^{-5}$ – $10^{-4}$  M constant concentration) with cavitands **2d** and **2e** ( $10^{-4}$ – $5 \times 10^{-3}$  M concentration). This is in agreement with the previous complexation studies between fullerenes and calixarenes, see ref 24.

(24) For extensive studies on complexation of  $\text{C}_{60}$  and larger fullerenes by calixarenes in organic solvents, see: (a) Araki, K.; Akao, K.; Ikeda, A.; Suzuki, T.; Shinkai, S. *Tetrahedron Lett.* **1996**, *37*, 73–76. (b) Ikeda, A.; Yoshimura, M.; Shinkai, S. *Tetrahedron Lett.* **1997**, *38*, 2107–2110. (c) Haino, T.; Yanase, M.; Fukazawa, Y. *Angew. Chem., Int. Ed. Engl.* **1997**, *36*, 259–260. (d) Haino, T.; Yanase, M.; Fukazawa, Y. *Angew. Chem., Int. Ed. Engl.* **1998**, *37*, 997–998. (e) Ikeda, A.; Suzuki, Y.; Yoshimura, M.; Shinkai, S. *Tetrahedron* **1998**, *54*, 2497–2508.

(25) The only known example in resorcinarene host–guest chemistry was reported by Aoyama et al.: (a) Kikuchi, Y.; Kato, Y.; Tanaka, Y.; Toi, H.; Aoyama, Y. *J. Am. Chem. Soc.* **1991**, *113*, 1349–1354. (b) Kobayashi, K.; Asakawa, Y.; Kikuchi, Y.; Toi, H.; Aoyama, Y. *J. Am. Chem. Soc.* **1993**, *115*, 2648–2654. Slow exchange (on the NMR time scale) between complexed and free guest and significant complexation-induced upfield shifts of the  $^1\text{H}$  NMR signals for bound guest due to the ring-current effects of the host aromatics were found even upon very weak complexation ( $K_{\text{ass}} \leq 10 \text{ M}^{-1}$ ). The resorcinarene OH groups as well as CH- $\pi$  interaction were responsible for the complexation. For the review, see: Aoyama, Y. In *Comprehensive Supramolecular Chemistry*, Vögtle, F., Ed.; Pergamon: Elmsford, NY, 1996; Vol. 2, p 279–307.

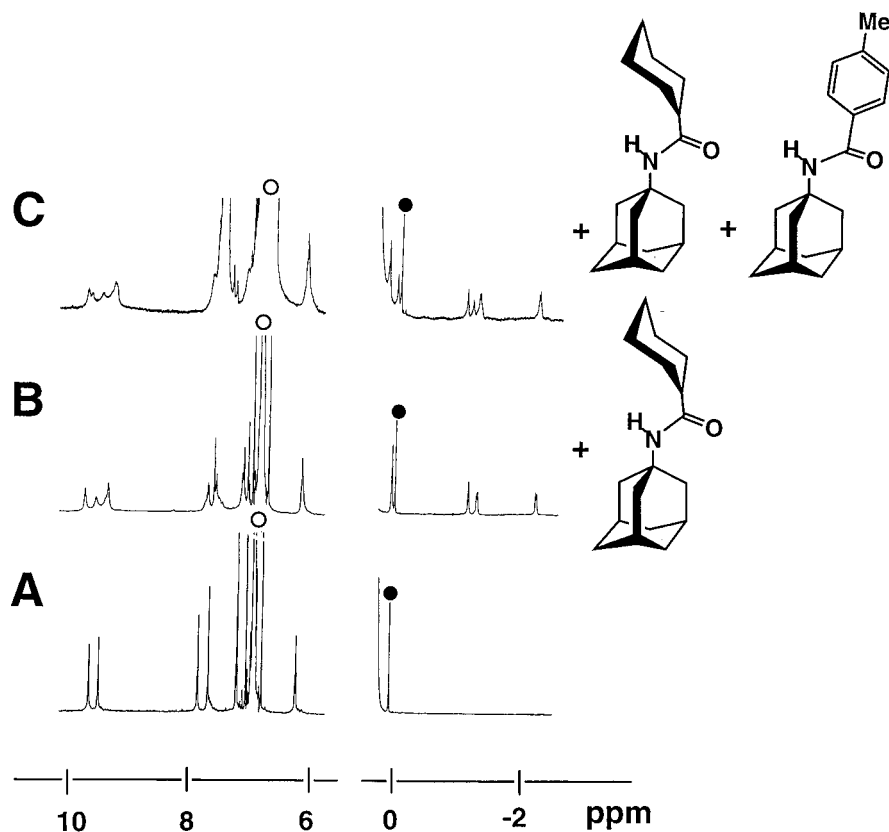


**Figure 10.** Upfield and downfield regions of  $^1\text{H}$  NMR spectra (*p*-xylene- $d_{10}$ , 600 MHz, 295 K) of: (A) Cavitand **2e**. (B) The complex with *N*-(1-adamantyl)-cyclohexanecarboxamide. (C) The mixture of two different complexes, with *N*-(1-adamantyl)cyclohexanecarboxamide and *N*-(1-adamantyl)-*p*-toluylamide. The **2e** concentration was 0.5 mM, and the guest concentration is ca. 50 mM. Residual signals of guest-free cavitand **2e** are also present due to weak complexation. The solvent signals with corresponding satellites and the internal standard singlet are marked as before.

NMR shifts of the complexed molecules offered the possibility to examine the structural details of the complexes “from inside”, that is, to determine the orientation of the guest and its interaction with the receptor walls inside the cavity. In addition, it was possible to determine how the macroscopic environment (e.g., bulk solution, concentration or temperature changes, etc.) influence the shielded complexed species. The self-folding cavitands are in an unusual position in the scale of cavity-containing receptors. Even though the guest exchange process is slow on the NMR time scale ( $k = 2 \pm 1 \text{ s}^{-1}$ ), it is still faster than that observed for the completely closed hydrogen-bonded calixarene-based capsule ( $k \leq 0.47 \pm 0.1 \text{ s}^{-1}$ )<sup>26</sup> or for covalently bound hemicarcerands ( $k = 0.0093 \text{ s}^{-1}$ ).<sup>27</sup>

**Orientation inside the Cavity.** Previously, the guest positioning inside cavitands was determined exclusively in the solid state by X-ray crystallography.<sup>1,7,8</sup> Due to the fast complexation–decomplexation process on the NMR time scale, the chemical shift changes report an average of many environments and are not always easily interpreted. Soncini and Dalcanale explained the upfield shift of  $\text{NMe}_2$  in the complex **3** ( $\text{R} = (\text{CH}_2)_5\text{CH}_3$ )-*p*-nitro-*N,N*-dimethylaniline by an orientation, wherein the  $\text{NMe}_2$  is deep inside the cavity, in acetone- $d_6$  solution.<sup>7</sup> Reinhoudt et al. deduced the structure of some steroid complexes by systematic  $^1\text{H}$  NMR studies, employing various model host and guest compounds.<sup>5</sup> In contrast, for the complexes of self-folding cavitands **2a–e**, the  $^1\text{H}$  NMR solution spectra speak for themselves.

Integration clearly indicates that only one guest molecule is accommodated inside the deep cavity, a stoichiometry anticipated by molecular modeling.<sup>16</sup> The association constant values  $K_{\text{ass}}$  of  $400 \pm 100 \text{ M}^{-1}$  ( $-\Delta G^\circ = 3.5 \pm 0.2 \text{ kcal mol}^{-1}$ ) for *N*-cyclohexyluracil **8**,  $850 \pm 25 \text{ M}^{-1}$  ( $-\Delta G^\circ = 3.9 \text{ kcal mol}^{-1}$ ) for  $\epsilon$ -caprolactam **9b**, and  $40 \pm 10 \text{ M}^{-1}$  ( $-\Delta G^\circ = 2.0 \pm 0.3 \text{ kcal mol}^{-1}$ )<sup>12</sup> for adamantanes **12,13** were obtained directly from the integration of the NMR spectra at 295 K in *p*-xylene- $d_{10}$ . However, in benzene- $d_6$  and  $\text{CDCl}_3$  the binding affinities were an order of magnitude lower, and  $-\Delta G^\circ$  values of  $0.5 \pm 0.1 \text{ kcal mol}^{-1}$  at 295 K were found for adamantanes **12,13**; no kinetically stable complex with **8** was detected in  $\text{CDCl}_3$ . Apparently, some guests have difficulties competing with the high concentrations of solvents for the interior of the cavity, but even then the barriers to exchange remain high. At higher temperatures ( $\geq 60 \text{ }^\circ\text{C}$ ), the signals for complexed and free species become broad, and the guest signals eventually disappear into the baseline.

The NOESY spectrum of the **2d**•adamantane complex showed NOE connectivities between the signals of the complexed adamantane with the signals for the N–H and the catechol aromatic protons. Accordingly, the guest molecule floats in the cavity above the resorcinarene platform (Figure 7B), as anticipated by the solid-state structures of known caviplexes.<sup>7</sup>

For the complexed 1-substituted adamantanes, all three sets of the skeleton protons can be clearly seen (Figures 9 and 10). Due to the effects of the nearby aromatic ring-currents, the chemical shifts of the guest signals are directly related to their position inside the cavity. The functional group at the adamantane 1-position is generally not shifted upfield in the NMR

(26) Mogck, O.; Pons, M.; Böhmer, V.; Vogt, W. *J. Am. Chem. Soc.* **1997**, *119*, 5706–5712.

(27) Cram, D. J.; Blanda, M. T.; Paek, K.; Knobler, C. B. *J. Am. Chem. Soc.* **1992**, *114*, 7765–7773.



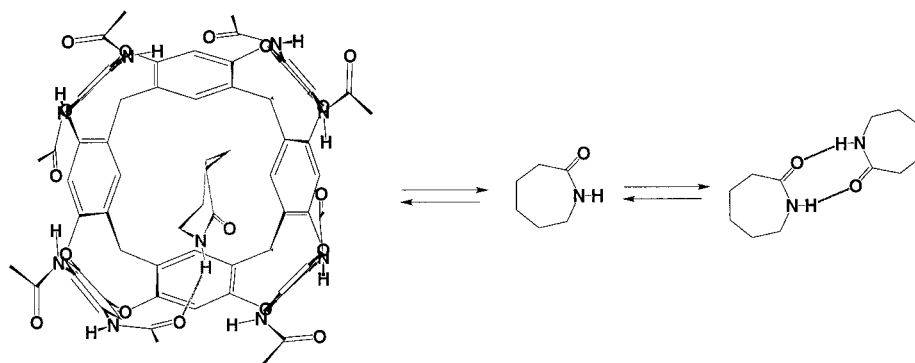


**Figure 11.** Dimerization of  $\epsilon$ -caprolactam in an apolar solvent and the energy-minimized<sup>16</sup> structure of its complex with cavitand **2**. Long alkyl chains and CH hydrogens are omitted.

spectra, indicating that the adamantane skeleton is oriented toward the bottom of the cavity and the functional group toward the top. One exception was the case of 1-adamantanamine, where the  $\text{NH}_2$ -group is situated deeply inside the cavity and the  $\text{NH}_2$  resonance is the signal most shielded and appears at  $-2$  ppm. The pattern of signals for the C–H resonances is also reversed in this case (Figure 9C). Apparently, the interaction of the weakly acidic  $\text{NH}_2$  hydrogens with the  $\pi$ -surface of the resorcinarene is enough to favor this orientation over others which offer only CH- $\pi$  interactions.

1-[N-(1-Adamantyl)]adamantanecarboxamide, taken in ca. 50-fold excess, gave two diastereomeric 1:1 complexes with **2d,e** in *p*-xylene- $d_{10}$  solution (Figure 9D); two sets of characteristically upfield adamantane signals can be seen. Both adamantyl ends have approximately the same affinity toward the receptor cavity, as can be concluded from the integration. The adamantane guest can spin about the long axis of the cavity but is too large to tumble within it. The resulting diastereomerism has precedent in carceplexes<sup>28</sup> but was unknown in open-ended cavities. In the cases of *N*-cyclohexyluracil **8** and lactams **9b,c**, **10**, and **11**, most of the cycloalkyl signals of the encapsulated guest are broad at 295 K and situated between 0.5 and  $-3$  ppm (see also Figure 8A,B). The broadening may indicate the effects of the reduced symmetry of the guests inside the circle of amides and a reduced tumbling of these guests.

**Hydrogen Bonding in a Shielded Environment.** When molecules possessing hydrogen bonding sites are placed inside the cavity, they have the occasion to interact with each other and/or with the walls, and these interactions can be strong or weak.<sup>29</sup> Lactams are known to dimerize in apolar solvents through hydrogen bonding, and typical dimerization constant values are usually 20–45  $\text{M}^{-1}$  in benzene and 100–150  $\text{M}^{-1}$  in  $\text{CCl}_4$ .<sup>30</sup> We showed that cavitands **2d,e** encapsulate lactams, namely  $\epsilon$ -caprolactam **9b**, *N*-methylcaprolactam **10**, 2-azacylononanone **9c**, 7-butyltetrahydro-2(3H)-azepinone **11**, and 4-azatricyclo[4.3.1.1<sup>3,8</sup>]undecan-5-one **13** (Figures 7 and 8B).

(28) (a) Timmerman, P.; Verboom, W.; van Veggel, F. C. J. M.; van Duynhoven, J. P. M.; Reinhoudt, D. N. *Angew. Chem., Int. Ed. Engl.* **1994**, *33*, 2345–2348. (b) Chapman, R. G.; Sherman, J. C. *J. Am. Chem. Soc.* **1995**, *117*, 9081–9082. For self-assembled capsules, see ref 11a.

(29) For earlier studies of hydrogen bonding inside synthetic (assembled) niches, see: (a) Nowick, J. S.; Chen, J. S.; Noronha, G. *J. Am. Chem. Soc.* **1993**, *115*, 7636–7644. (b) Nowick, J. S.; Cao, T.; Noronha, G. *J. Am. Chem. Soc.* **1994**, *116*, 3285–3289. (c) Ruf, M.; Weis, K.; Vahrenkamp, H. *Inorg. Chem.* **1997**, *36*, 2130–2137. (d) Zimmerman, S. C.; Wang, Y.; Bharathi, P.; Moore, J. S. *J. Am. Chem. Soc.* **1998**, *120*, 2172–2173.

(30) (a) Klemperer, W.; Cronyn, M. W.; Maki, A. H.; Pimentel, G. C. *J. Am. Chem. Soc.* **1954**, *76*, 5846–5848. (b) Huisgen, R.; Walz, H. *Chem. Ber.* **1956**, *89*, 2616–2629. (c) Hopmann, R. F. W. *J. Phys. Chem.* **1974**, *78*, 2341–2348. (d) Wagner, K.; Rudakoff, G.; Frölich, P. *Z. Chem.* **1975**, *15*, 272–275. (e) Walmsley, J. A. *J. Phys. Chem.* **1978**, *82*, 2031–2035. (f) Krikorian, S. E. *J. Phys. Chem.* **1982**, *86*, 1875–1881.

Smaller lactams, such 2-pyrrolidinone and valerolactam **9a**, did not show kinetically stable inclusion.

We then probed  $\epsilon$ -caprolactam **9b** dimerization properties within the complex of **2d,e**.<sup>31</sup> It was first determined that  $\epsilon$ -caprolactam dimerizes in *p*-xylene- $d_{10}$  with  $K_D = 50 \pm 10 \text{ M}^{-1}$  ( $-\Delta G^\circ = 2.3 \text{ kcal mol}^{-1}$ ), a value in good agreement with the previously published figures in similar solvents.<sup>30</sup> All six groups of protons changed their position upon dilution. Specifically, changing the caprolactam concentration from ca. 95 mM to 0.7 mM caused an upfield shift of the NH signal from 7.3 to 4.9 ppm; the  $\text{CH}_2\text{NH}$  multiplet shifted from ca. 2.7 to 2.3 ppm upfield. Upon addition of caprolactam to the *p*-xylene- $d_{10}$  solution of cavitand **2d**, both free and encapsulated species can be clearly seen in the  $^1\text{H}$  NMR spectrum (Figure 8B), and the association constant  $K_a$  of  $850 \pm 25 \text{ M}^{-1}$  was calculated, assuming a 1:1 complex. Surprisingly, no changes in chemical shift for the encapsulated  $\epsilon$ -caprolactam molecules were detected upon ca. 160-fold change of the total caprolactam concentration (0.6–95 mM). This suggested that caprolactam does not form dimers inside the cavity **2d**; rather, the complexed  $\epsilon$ -caprolactam molecule is shielded from those in bulk solution. The role of the long chains on the amide functions have yet to be defined in this context. In addition, hydrogen bonding is possible between the  $\epsilon$ -caprolactam as a donor (or acceptor) and any of the **2d** (wall) amide groups (see Figure 11). This likely further protects the lactam from the environment outside. Such hydrogen bonding was suggested by molecular modeling<sup>16</sup> and by a competition experiment. When a 1:1 mixture of caprolactam **9b** and the acceptor but not donor, *N*-methylcaprolactam **10**, (ca. 40 mM each) was added to the 0.5 mM *p*-xylene- $d_{10}$  solution of cavitand **2d**, the **9b**·**2d** complex was observed predominantly (>90%).

In conclusion, self-folding cavitands represent a new species of molecular containers, distinct from the covalently sealed carcerands and the reversibly formed hydrogen-bonded capsules. The “self” refers to the effects of the hydrogen bonds on the behavior of the molecules and is also the popular prefix for molecular recognition phenomena of the decade: replication, assembly, and organization. The deep cavities here are open, but guest inclusion is slow on the NMR time scale. The uptake and release of guests involves the folding and unfolding of the host, achieved by either varying solvent polarity and/or temperature. There is a possibility of using these containers as

(31) Cram has described a carceplex with 2-pyrrolidinone and suggested hydrogen bonding occurs between the guest NH and the inward-turned unshared electron pairs of the host  $\text{ArOCH}_2$  walls. This orients the 2-pyrrolidinone cycle to the equatorial region of the carceplex cavity. See: Robbins, T. A.; Knobler, C. B.; Bellow, D. R.; Cram, D. J. *J. Am. Chem. Soc.* **1994**, *116*, 111–122.



reaction vessels for monosubstituted adamantane derivatives since the corresponding acid chloride, amine, and isocyanate are easily accommodated inside (Figure 7). As the constant flow of the substrate into and the product out of the cavity can be envisioned, turnover and true catalysis may be possible. The introduction of additional (catalytically) useful sites on the upper rim would also appear likely. The most immediate application is in analysis. Cavitands **2** act as NMR shift reagents for number of molecules, substituted adamantanes, lactams, and cyclohexane derivatives. Their  $^1\text{H}$  NMR spectra as mixtures can be easily analyzed in the upfield (negative ppm region) but not in their usual regions because of overlapping resonances. For example, Figure 10C shows how the distribution of two monosubstituted adamantanes inside a cavity can be determined using only 1–2 mol % of **2e** as a shift reagent. We are currently exploring these applications and will report on them in due course.

## Experimental Section

**General.** Melting points were determined on a Thomas-Hoover capillary melting point apparatus and are uncorrected.  $^1\text{H}$  NMR and  $^{13}\text{C}$  NMR spectra were recorded on a Bruker AM-300 and a Bruker DRX-600 spectrometers. The chemical shifts were measured relative to residual nondeuterated solvent resonances or TMS. Fast atom bombardment (FAB) mass-spectra were obtained with a VG ZAB-VSE double focusing high-resolution mass spectrometer equipped with a cesium ion gun; *m*-nitrobenzyl alcohol (NBA) was used as a matrix. For high-resolution mass spectral data (HRMS-FAB), for compounds with molecular weight  $\leq 500$ , the measured masses always agreed to  $\leq 5$  ppm with the calculated values. For compounds with significantly higher molecular weight ( $\geq 2000$ ), lower resolution was achieved.<sup>32</sup> In most of the cases, the FAB-MS measurements were taken in duplicate. Matrix-assisted laser desorption/ionization (MALDI) mass spectrometry experiments were performed on a PerSeptive Biosystems Voyager-Elite mass spectrometer with delayed extraction, using 2,5-dihydroxybenzoic acid (DHB) as a matrix. Electrospray ionization (ESI) mass spectra were recorded on an API III Perkin-Elmer SCIEX triple quadrupole mass spectrometer. FTIR spectra were recorded on a Perkin-Elmer Paragon 1000 PC FT-IR spectrometer. Silica gel chromatography was performed with Silica Gel 60 (EM Science or Bodman, 230–400 mesh). All experiments with moisture- or air-sensitive compounds were performed in anhydrous solvents under a nitrogen atmosphere. Compounds **1a–c**<sup>1b,1c</sup> and **3** ( $\text{R} = (\text{CH}_2)_{10}\text{CH}_3$ )<sup>7</sup> were synthesized in accordance with the literature protocols. Molecular modeling was performed using the Amber\* force field in the MacroModel 5.5 program.<sup>16</sup>

**General Procedure for the Preparation of Octaamides 2a–e and 5, and Heptaamides 6.** A mixture of octanitro compound **4a–c** (0.12 mmol) and  $\text{SnCl}_2 \cdot 2\text{H}_2\text{O}$  (1 g, 4.4 mmol) was boiled in 20 mL of EtOH and concentrated HCl (3–5 mL) for 5 h, cooled, and then poured onto ice. The pH was adjusted to 10 with 2 M aqueous NaOH, and the released octaamine was extracted with  $\text{CH}_2\text{Cl}_2$  ( $2 \times 50$  mL). The organic layer was washed with water ( $2 \times 100$  mL), dried over  $\text{Na}_2\text{SO}_4$ , and then evaporated to give the octaamines as greenish solids. These were used immediately for the next step. The yields were 60–65%, and the crude octaamines gave satisfactory mass-spectral data.

To a vigorously stirred mixture of the appropriate octaamine (0.08 mmol) and  $\text{K}_2\text{CO}_3$  (0.1 g, 0.65 mmol) in  $\text{EtOAc-H}_2\text{O}$ , 1:1 (20 mL) was added the specified acid chloride (0.65 mmol) by syringe. The reaction mixture was stirred for 2 h, the organic layer was separated, and the aqueous layer was extracted with  $\text{CH}_2\text{Cl}_2$  ( $2 \times 25$  mL). The combined organic layers were washed with water ( $2 \times 100$  mL), dried over  $\text{MgSO}_4$ , and then evaporated. Pure amides **2a–e** and **5** were obtained as colorless solids in 50–55% yields by preparative TLC (silica gel) using  $\text{EtOAc-hexanes}$  mixtures. Heptaamides **6a,b** were isolated as byproducts in ca. 10% yield through preparative TLC.

(32) For technical details on high-resolution mass spectrometry, see: (a) Rose, M. E.; Johnstone, R. A. W. *Mass Spectrometry for Chemists and Biochemists*; Cambridge University Press: Cambridge, 1982. (b) Jennings, K. R.; Dolnikowski, G. G. In *Methods in Enzymology*; McCloskey, J. A., Ed.; Academic Press: New York, 1990; p 37 and references therein.

**27,37:28,36-Dimetheno-29H,31H,33H,35H-dibenzo[*b,b'*]bis[1,7]-benzodioxonino[3,2-*j*:3',2'-*j'*]benzo[1,2-*e*:5,4-*e'*]bis[1,3]-benzodioxonin, 2,3,9,10,16,17,23,24-octakis(*n*-octanoylamido)29,31,33,35-tetranonyl- (2a):** colorless foam;  $^1\text{H}$  NMR (benzene- $d_6$ )  $\delta$  10.02, 9.85 ( $2 \times s$ , 8 H), 8.01, 7.78, 7.47, 7.31 ( $4 \times s$ , 16 H), 6.36 (t,  $J = 8.2$  Hz, 4 H), 2.6–2.1, 1.8–1.4, 1.3–1.1 (m, 160 H), 0.99 (t,  $J = 7.0$  Hz, 12 H), 0.94 (t,  $J = 7.0$  Hz, 24 H); HRMS-FAB  $m/z$  2550.6284 ( $[\text{M} + \text{Cs}]^+$ , calcd for  $\text{C}_{152}\text{H}_{224}\text{N}_8\text{O}_{16}\text{Cs}$  2550.6015).

**27,37:28,36-Dimetheno-29H,31H,33H,35H-dibenzo[*b,b'*]bis[1,7]-benzodioxonino[3,2-*j*:3',2'-*j'*]benzo[1,2-*e*:5,4-*e'*]bis[1,3]-benzodioxonin, 2,3,9,10,16,17,23,24-octakis(cyclohexanoylamido)29,31,33,35-tetranonyl- (2b):** mp  $> 175$  °C dec;  $^1\text{H}$  NMR (benzene- $d_6$ )  $\delta$  9.85, 9.46 ( $2 \times s$ , 8 H), 7.94, 7.73, 7.38, 7.35 ( $4 \times s$ , 16 H), 6.30 (t,  $J = 8.2$  Hz, 4 H), 2.4–1.1 (m, 168 H), 0.93 (t,  $J = 7.0$  Hz, 12 H); HRMS-FAB  $m/z$  2422.3696 ( $[\text{M} + \text{Cs}]^+$ , calcd for  $\text{C}_{144}\text{H}_{192}\text{N}_8\text{O}_{16}\text{Cs}$  2422.3511).

**27,37:28,36-Dimetheno-29H,31H,33H,35H-dibenzo[*b,b'*]bis[1,7]-benzodioxonino[3,2-*j*:3',2'-*j'*]benzo[1,2-*e*:5,4-*e'*]bis[1,3]-benzodioxonin, 2,3,9,10,16,17,23,24-octakis(chloroacetyl-amido)29,31,33,35-tetranonyl- (2c):** mp  $> 195$  °C dec;  $^1\text{H}$  NMR ( $\text{CDCl}_3$ )  $\delta$  9.54 (s, 8 H), 7.56 (s, 8 H), 7.30, 7.20 ( $2 \times s$ , 8 H), 5.77 (t,  $J = 8.0$  Hz, 4 H), 4.21, 4.10 ( $2 \times d$ ,  $J = 13.6$  Hz, 16 H), 2.25 (m, 8 H), 1.3 (m, 56 H), 0.91 (t,  $J = 7.2$  Hz, 12 H);  $^1\text{H}$  NMR (benzene- $d_6$ )  $\delta$  9.58 (s, 8 H), 7.75, 7.00 ( $2 \times s$ , 8 H), 7.26 (s, 8 H), 6.28 (t,  $J = 8.0$  Hz, 4 H), 3.58, 3.49 ( $2 \times d$ ,  $J = 13.7$  Hz, 16 H), 2.42 (m, 8 H), 1.5, 1.4, 1.3 ( $3 \times m$ , 56 H), 0.93 (t,  $J = 7.2$  Hz, 12 H); HRMS-FAB  $m/z$  2149.5553 ( $[\text{M} + \text{Cs}]^+$ , calcd for  $\text{C}_{104}\text{H}_{120}\text{Cl}_8\text{N}_8\text{O}_{16}\text{Cs}$  2149.5385).

**27,37:28,36-Dimetheno-29H,31H,33H,35H-dibenzo[*b,b'*]bis[1,7]-benzodioxonino[3,2-*j*:3',2'-*j'*]benzo[1,2-*e*:5,4-*e'*]bis[1,3]-benzodioxonin, 2,3,9,10,16,17,23,24-octakis(*n*-octano-ylamido)29,31,33,35-tetraundecyl- (2d):** mp 239–240 °C;  $^1\text{H}$  NMR ( $\text{CDCl}_3$ )  $\delta$  9.90, 9.09 ( $2 \times s$ , 8 H), 7.77, 7.20, 7.12, 7.09 ( $4 \times s$ , 16 H), 5.79 (t,  $J = 8.1$  Hz, 4 H), 2.6–1.2 (m, 168 H), 1.0–0.9 (m, 36 H);  $^1\text{H}$  NMR (benzene- $d_6$ )  $\delta$  10.06, 9.86 ( $2 \times s$ , 8 H), 8.00, 7.78, 7.47, 7.30 ( $4 \times s$ , 16 H), 6.37 (t,  $J = 8.2$  Hz, 4 H), 2.58, 2.45, 2.42, 2.25, 2.11, 1.75, 1.65, 1.5, 1.4, 1.3–1.1 ( $12 \times m$ , 176 H), 1.00 (t,  $J = 7.0$  Hz, 12 H), 0.96 (t,  $J = 7.0$  Hz, 24 H);  $^1\text{H}$  NMR (*p*-xylene- $d_{10}$ )  $\delta$  10.02, 9.82 ( $2 \times s$ , 8 H), 8.00, 7.78, 7.47, 7.30 ( $4 \times s$ , 16 H), 6.37 (t,  $J = 8.2$  Hz, 4 H), 2.58, 2.45, 2.42, 2.25, 2.11, 1.75, 1.65, 1.5, 1.4, 1.3–1.1 ( $12 \times m$ , 176 H), 1.00 (t,  $J = 7.0$  Hz, 12 H), 0.96 (t,  $J = 7.0$  Hz, 24 H);  $^1\text{H}$  NMR (mesitylene- $d_{12}$ )  $\delta$  9.79, 9.33 ( $2 \times s$ , 8 H), 7.91, 7.63, 7.21, 7.13 ( $4 \times s$ , 16 H), 6.16 (t,  $J = 8.2$  Hz, 4 H), 2.5–1.2 (m, 176 H), 0.98 (t,  $J = 7.0$  Hz, 12 H), 0.96 (t,  $J = 7.0$  Hz, 24 H); MALDI-MS  $m/z$  2553 ( $[\text{M} + \text{Na}]^+$ , calcd 2553); HRMS-FAB  $m/z$  2663.7505 ( $[\text{M} + \text{Cs}]^+$ , calcd for  $\text{C}_{160}\text{H}_{240}\text{N}_8\text{O}_{16}\text{Cs}$  2662.7267).

**27,37:28,36-Dimetheno-29H,31H,33H,35H-dibenzo[*b,b'*]bis[1,7]-benzodioxonino[3,2-*j*:3',2'-*j'*]benzo[1,2-*e*:5,4-*e'*]bis[1,3]-benzodioxonin, 2,3,9,10,16,17,23,24-octakis(cyclohexa-noylamido)29,31,33,35-tetraundecyl- (2e):** mp 108 °C dec;  $^1\text{H}$  NMR (benzene- $d_6$ )  $\delta$  9.84, 9.37 ( $2 \times s$ , 8 H), 7.93, 7.75, 7.41, 7.29 ( $4 \times s$ , 16 H), 6.32 (t,  $J = 8.1$  Hz, 4 H), 2.4–1.1 (m, 168 H), 0.93 (t,  $J = 7.0$  Hz, 12 H);  $^1\text{H}$  NMR (*p*-xylene- $d_{10}$ )  $\delta$  9.55, 9.48 ( $2 \times s$ , 8 H), 7.83, 7.66, 7.18, 7.03 ( $4 \times s$ , 16 H), 6.21 (t,  $J = 8.2$  Hz, 4 H), 2.4–1.1 (m, 168 H), 0.97 (t,  $J = 7.0$  Hz, 12 H); MALDI-MS  $m/z$  2425 ( $[\text{M} + \text{Na}]^+$ , calcd 2425); HRMS-FAB  $m/z$  2535.4911 ( $[\text{M} + \text{Cs}]^+$ , calcd for  $\text{C}_{152}\text{H}_{208}\text{N}_8\text{O}_{16}\text{Cs}$  2534.4763).

**27,37:28,36-Dimetheno-29H,31H,33H,35H-dibenzo[*b,b'*]bis[1,7]-benzodioxonino[3,2-*j*:3',2'-*j'*]benzo[1,2-*e*:5,4-*e'*]bis[1,3]-benzodioxonin, 6,13,20,39-tetramethyl-2,3,9,10,16,17,23,24-octakis(*n*-octanoylamido)29,31,33,35-tetranonyl- (5):** foamed;  $^1\text{H}$  NMR ( $\text{DMSO-CDCl}_3$ , 10:1)  $\delta$  9.18, 9.11 ( $2 \times s$ , 8 H), 7.46, 6.87 ( $2 \times s$ , 8 H), 6.91, 6.03 ( $2 \times s$ , 4 H), 3.93 (m, 4 H), 2.24, 2.04 ( $2 \times s$ , 12 H), 2.5–2.3, 2.3–2.0, 1.9–1.7, 1.3–1.1 (m, 160 H), 0.90 (t,  $J = 7.0$  Hz, 12 H), 0.83 (t,  $J = 7.0$  Hz, 24 H); HRMS-FAB  $m/z$  2606.6363 ( $[\text{M} + \text{Cs}]^+$ , calcd for  $\text{C}_{156}\text{H}_{232}\text{N}_8\text{O}_{16}\text{Cs}$  2606.6641).

**27,37:28,36-Dimetheno-29H,31H,33H,35H-dibenzo[*b,b'*]bis[1,7]-benzodioxonino[3,2-*j*:3',2'-*j'*]benzo[1,2-*e*:5,4-*e'*]bis[1,3]-benzodioxonin, 2-amino-3,9,10,16,17,23,24-heptakis-(chloroacetyl-amido)29,31,33,35-tetranonyl- (6a):** mp 165 °C dec;  $^1\text{H}$  NMR (benzene- $d_6$ )  $\delta$  9.98, 9.82, 9.59, 9.55, 9.51, 9.07, 8.34 ( $7 \times s$ , 7 H), 7.8–7.4 ( $8 \times s$ , 8 H), 7.2–7.0 (m, 8 H), 6.44, 6.39, 6.08, 6.03 ( $4 \times t$ ,  $J = 8.2$  Hz, 4 H), 3.8–3.5 (m, 16 H), 2.4–2.2, 1.6–1.2, 1.0–0.9 (m,

76 H); HRMS-FAB  $m/z$  2073.5504 ( $[M + Cs]^+$ , calcd for  $C_{102}H_{119}-Cl_7N_8O_{15}Cs$  2073.5669).

**27,37:28,36-Dimetheno-29H,31H,33H,35H-dibenzo[*b,b'*]bis[1,7]-benzodioxonino[3,2-*j*:3',2'-*j'*]benzo[1,2-*e*:5,4-*e'*]bis[1,3]-benzodioxonin, 2-amino-3,9,10,16,17,23,24-heptakis-(*n*-octanoylamido)29,31,33,35-tetraundecyl- (6b):** mp 200–205 °C;  $^1H$  NMR (330 K,  $CDCl_3$ )  $\delta$  9.49, 9.37, 9.22, 9.12 (4  $\times$  s, 4 H), 9.26, 8.49, 8.13 (3  $\times$  br s, 3 H), 7.73, 7.67 (2  $\times$  s, 2 H), 7.5–7.3 (m, 14 H), 5.82, 5.71 (4  $\times$  t,  $J = 8.1$  Hz, 4 H), 2.3–2.1, 1.8–1.7, 1.4–1.2, 1.0–0.9 (4  $\times$  m, 212 H);  $^1H$  NMR (330 K, benzene- $d_6$ )  $\delta$  9.80, 9.74, 9.66, 9.58, 9.50 (5  $\times$  s, 5 H), 9.22, 8.63 (2  $\times$  br s, 2 H), 8.0–7.9, 7.77, 7.73, 7.71, 7.69, 7.68, 7.41, 7.28, 7.27, 7.17 (m and 9  $\times$  s, 16 H), 6.39, 6.35, 6.14, 6.11 (4  $\times$  t,  $J = 8.1$  Hz, 4 H), 2.4–2.1, 2.0–1.7, 1.5–1.2, 1.0–0.9 (4  $\times$  m, 212 H); HRMS-FAB  $m/z$  2536.6418 ( $[M + Cs]^+$ , calcd for  $C_{152}H_{226}-N_8O_{15}Cs$  2536.6222).

**General Procedure for the Preparation of Octanitro Compounds 4a–c.** To a solution of resorcinarene **1a–c** (1 mmol) and 1,2-difluoro-4,5-dinitrobenzene<sup>17</sup> (0.9 g, 4.4 mmol) in DMA (20 mL) was added  $Et_3N$  (1.3 mL). The solution was heated at 120 °C for 4–5 h, cooled, and diluted with water (300–400 mL). The precipitate was filtered off, washed with water (3  $\times$  100 mL), and dried. The products were purified by column chromatography with  $CH_2Cl_2$  as an eluent and precipitated with cold MeOH. The yellow solids were obtained in 25–40% yields.

**27,37:28,36-Dimetheno-29H,31H,33H,35H-dibenzo[*b,b'*]bis[1,7]-benzodioxonino[3,2-*j*:3',2'-*j'*]benzo[1,2-*e*:5,4-*e'*]bis[1,3]-benzodioxonin, 2,3,9,10,16,17,23,24-octanitro-29,31,33,35-tetraundecyl- (4a):** mp >250 °C dec;  $^1H$  NMR ( $CDCl_3$ , 295 K)  $\delta$  7.66, 7.61 (2  $\times$  s, 8 H), 7.25, 6.20 (2  $\times$  s, 4 H), 7.10, 7.08 (2  $\times$  s, 4 H), 3.90 (m, 4 H), 2.1, 2.0 (2  $\times$  m, 8 H), 1.4–1.2 (m, 56 H), 0.87 (t,  $J = 7.2$  Hz, 12 H); ESI-MS  $m/z$  1648 ( $[M + H]^+$ , calcd for  $C_{88}H_{96}N_8O_{24}$  1649).

**27,37:28,36-Dimetheno-29H,31H,33H,35H-dibenzo[*b,b'*]bis[1,7]-benzodioxonino[3,2-*j*:3',2'-*j'*]benzo[1,2-*e*:5,4-*e'*]bis[1,3]-benzodioxonin, 6,13,20,39-tetramethyl-2,3,9,10,16,17,23,24-octanitro-29,31,33,35-tetraundecyl- (4b).** The compound is structurally similar to the previously prepared by Cram.<sup>4</sup> Mp >350 °C;  $^1H$  NMR ( $CDCl_3$ , 295 K)  $\delta$  7.78, 7.48 (2  $\times$  s, 8 H), 7.08, 5.97 (2  $\times$  s, 4 H), 3.87 (m, 4 H), 2.40, 2.21 (2  $\times$  s, 12 H), 2.2–2.0 (2  $\times$  m, 8 H), 1.5–1.2 (m, 56 H), 0.84 (t,  $J = 7.0$  Hz, 12 H); MS-FAB  $m/z$  1838 ( $[M + Cs]^+$ , calcd for  $C_{92}H_{104}N_8O_{24}Cs$  1838).

**27,37:28,36-Dimetheno-29H,31H,33H,35H-dibenzo[*b,b'*]bis[1,7]-benzodioxonino[3,2-*j*:3',2'-*j'*]benzo[1,2-*e*:5,4-*e'*]bis[1,3]-benzodioxonin, 2,3,9,10,16,17,23,24-octanitro-29,31,33,35-tetraundecyl- (4c):** mp >350 °C;  $^1H$  NMR ( $CDCl_3$ , 295 K)  $\delta$  7.66, 7.60 (2  $\times$  s, 8 H), 7.23, 6.22 (2  $\times$  s, 4 H), 7.10, 7.08 (2  $\times$  s, 4 H), 3.93 (m, 4 H), 2.1, 2.0 (2  $\times$  m, 8 H), 1.4–1.2 (m, 72 H), 0.89 (t,  $J = 7.2$  Hz, 12 H);  $^1H$  NMR ( $CDCl_3$ , 330 K)  $\delta$  7.63 (s, 8 H), 7.21, 6.22 (2  $\times$  br s, 4 H), 7.04 (s, 4 H), 3.95 (t,  $J = 7.6$  Hz, 4 H), 2.1, 2.0 (2  $\times$  m, 8 H), 1.4–1.2 (m, 72 H), 0.89 (t,  $J = 7.2$  Hz, 12 H); HRMS-FAB  $m/z$  1893.6656 ( $[M + Cs]^+$ , calcd for  $C_{96}H_{112}N_8O_{24}Cs$  1893.6844).

**General Procedure for the Preparation of Bis-amides 7a,b.** To a vigorously stirred mixture of 1,2-diamino-4,5-dimethoxybenzene<sup>19</sup> (0.34 g, 2 mmol) and  $K_2CO_3$  (0.69 g, 5 mmol) in  $EtOAc-H_2O$ , 1:1 (20 mL) was added the appropriate acid chloride (5 mmol) by syringe. The reaction mixture was stirred for 2 h, the organic layer was separated, and the aqueous layer was extracted with  $CH_2Cl_2$  (2  $\times$  25 mL). The combined organic layer was washed with water (2  $\times$  100 mL), dried over  $MgSO_4$ , and evaporated. Pure amides **7a,b** were obtained as tan solids in 75–85% yields after recrystallization from toluene.

**1,2-Dimethoxy-4,5-bis(*n*-octanoylamido)benzene (7a):** mp 140–141 °C;  $^1H$  NMR ( $CDCl_3$ )  $\delta$  8.2 (s, 2 H), 6.85 (s, 2 H), 3.82 (s, 6 H), 2.31 (t,  $J = 7.8$  Hz, 4 H), 1.7, 1.4, 1.3 (3  $\times$  m, 20 H), 0.90 (t,  $J = 7.1$  Hz, 6 H);  $^{13}C$  NMR ( $CDCl_3$ )  $\delta$  173.0, 147.4, 123.9, 105.0, 56.5, 37.5, 32.1, 29.7, 29.4, 26.2, 23.0, 14.5; HRMS-FAB  $m/z$  443.2873 ( $[M + Na]^+$ , calcd for  $C_{24}H_{40}N_8O_4Na$  443.2886).

**1,2-Dimethoxy-4,5-bis(chloroacetylamido)benzene (7b):** mp 185 °C;  $^1H$  NMR ( $CDCl_3$ )  $\delta$  8.6 (s, 2 H), 7.03 (s, 2 H), 4.22 (s, 4 H), 3.90 (s, 6 H);  $^{13}C$  NMR ( $CDCl_3$ )  $\delta$  165.6, 148.1, 122.8, 108.8, 56.6, 43.2; HRMS-FAB  $m/z$  321.0401 ( $[M + Na]^+$ , calcd for  $C_{12}H_{14}Cl_2N_8O_4Na$  321.0409).

**General Procedure for the Preparation of Adamantane Amides (12,13).** Amides **12**, **13** were prepared analogously to **7a,b** in 80–90% yields from the corresponding amines and acid chlorides, mixed

in a 1:1 molar ratio, under Schotten–Baumann conditions in  $EtOAc-H_2O$  in the presence of 2 equiv  $K_2CO_3$ .

**N-(1-Adamantyl)cyclohexanecarboxamide:** mp 190–191 °C (cyclohexane);  $^1H$  NMR (*p*-xylene- $d_{10}$ )  $\delta$  4.54 (br s, 1 H), 2.0–1.5 (mm, 26 H);  $^{13}C$  NMR ( $CDCl_3$ )  $\delta$  175.8, 51.8, 46.8, 42.1, 36.8, 30.2, 29.8, 26.2; HRMS-FAB  $m/z$  262.2169 ( $[M + Na]^+$ , calcd for  $C_{17}H_{27}NONa$  262.2171).

**N-(1-Adamantyl)toluoylcarboxamide:** mp 163 °C (toluene);  $^1H$  NMR (*p*-xylene- $d_{10}$ )  $\delta$  7.60, 7.00 (2  $\times$  d,  $J = 7.8$  Hz, 4 H), 5.42 (br s, 1 H), 2.10 (s, 3H), 2.0–1.5 (3  $\times$  m, 15 H);  $^{13}C$  NMR ( $CDCl_3$ )  $\delta$  167.0, 141.7, 133.5, 129.5, 127.2, 52.5, 42.1, 36.8, 29.9, 21.8; HRMS-FAB  $m/z$  270.1856 ( $[M + Na]^+$ , calcd for  $C_{18}H_{23}NONa$  270.1858).

**1-[N-(1-Adamantyl)]adamantanecarboxamide:** mp 315–316 °C ( $EtOH$ );  $^1H$  NMR (*p*-xylene- $d_{10}$ )  $\delta$  4.86 (br s, 1 H), 2.1–1.5 (5  $\times$  m, 30 H);  $^{13}C$  NMR ( $CDCl_3$ )  $\delta$  177.6, 51.6, 42.0, 41.2, 39.7, 36.8, 36.7, 29.7, 28.5; HRMS-FAB 314.2480 ( $[M + Na]^+$ , calcd for  $C_{21}H_{31}NONa$  314.2484).

**EXSY experiments.** The EXSY spectra of complex **2d**·adamantane were recorded at 295 K at 600 MHz with the phase sensitive NOESY pulse sequence supplied with the Bruker software. TPPI was used to obtain quadrature detection in  $F_1$ . Each of the 480  $F_1$  increments was the accumulation of 16 scans. The relaxation delay was 2.4 s. The mixing time was 500 ms. Before Fourier transformation, the FIDs were multiplied by a  $\pi/2$  shifted square sine bell function in both the  $F_2$  and the  $F_1$  domain. The data file was zero-filled, resulting in a spectrum of 4K  $\times$  1K real data points, with a resolution of 1.75 Hz/point in  $F_2$  and 7.03 Hz/point in  $F_1$ . The rate constants  $k$  were calculated from the measurements of the cross-peak ( $I_{AB}$ ,  $I_{BA}$ ) to diagonal peak intensities ( $I_{AA}$ ,  $I_{BB}$ ) and the molar fractions ( $X_A$ ,  $X_B$ ) of the different compounds undergoing exchange.

$$A \xrightleftharpoons[k_{-1}]{k_1} B$$

$$k = k_1 + k_{-1}$$

$$k = \frac{1}{t_m} \ln \frac{r+1}{r-1}$$

where  $r = 4X_A X_B (I_{AA} + I_{BB}) / (I_{AB} + I_{BA}) - (X_A - X_B)^2$

See also ref 33.

**$^1H$  NMR Binding Experiments.** Binding studies were performed at 295  $\pm$  1 K. The stoichiometry of complexation and the association constant  $K_{ass}$  values were determined in  $CDCl_3$ , benzene- $d_6$ , and *p*-xylene- $d_{10}$  at a constant (0.5–1.0 mM) concentration of host **2** and variable concentrations (1–100 mM) of a guest **8–14** by integration of the corresponding complex and free host signals. The concentration of complex formed was determined directly by referring to the integrals of the upfield shifted signals and the cavitand NH, aromatics, or methine CH signals.

For  $\epsilon$ -caprolactam **9b**, the dimerization constant  $K_D$  value was obtained in *p*-xylene- $d_{10}$  by simultaneously monitoring the NH,  $CH_2-NHC(O)$ , and  $CH_2C(O)NH$  chemical shifts at a concentration of 0.7–95 mM. The Horman–Dreux algorithm was employed in the calculations;<sup>34</sup> the nonspecific oligomerization<sup>30</sup> of  $\epsilon$ -caprolactam was neglected.

**Acknowledgment.** We are grateful to the Skaggs Research Foundation and the National Institutes of Health for support. The Wallenberg Foundation provided fellowship support to G.H. We also thank Dr. Emily Maverick of UCLA for advice and Ing. Ben Lammerink of Twente University for experimental assistance at the initial stage of this work.

**Supporting Information Available:** Representative  $^1H$  NMR spectra (12 pages, print/PDF). See any current masthead page for ordering information and Web access instructions.

JA982970G

(33) Perrin, C. L.; Dwyer, T. J. *Chem. Rev.* **1990**, *90*, 935–967.

(34) Horman, I.; Dreux, B. *Helv. Chim. Acta* **1984**, *67*, 754–764.